Numerical study of magnetic particles mixing in waste water under an external magnetic field

Christos Liosis, Evangelos G. Karvelas, Theodoros Karakasidis and Ioannis E. Sarris

ABSTRACT

The combination of nanotechnology and microfluidics may offer an effective water and wastewater treatment. A novel approach combines the use of magnetic particles which can capture heavy metal impurities in microfluidic ducts. The purpose of this study is to investigate the mixing mechanism of two water streams, one with magnetic particles and the other with wastewater. The optimum mixing is obtained when particles are uniformly distributed along the volume of water in the duct for the combined action of a permanent, spatially and temporally aligned magnetic field. Results showed that mixing is enhanced as the frequency of the magnetic field decreases or its amplitude increases, while magnetic gradient is found to play an insignificant role in the present configuration. Moreover, for simulations with low frequency, the mean concentration of particles is found to be twice as high as compared to the cases with higher frequency. Optimum distribution of particles inside the micromixer is observed for the combination of 0.6 T, 8 T/m and 5 Hz for the magnetic magnitude, gradient and frequency, respectively, where concentration reaches the optimal value of 0.77 mg/mL along the volume of the duct.

Key words | heavy metals, magnetic field, micromixer, particles, water treatment

Christos Liosis
Evangelos G. Karvelas
Theodoros Karakasidis (corresponding author)
Laboratory of Hydromechanics and Environmental Engineering, Department of Civil Engineering,
University of Thessaly,
38334 Volos,
Greece
E-mail: *thkarak@uth.gr*

Theodoros Karakasidis
Department of Physics,
University of Thessaly,
35100 Lamia,
Greece

Ioannis E. Sarris
Department of Mechanical Engineering,
University of West Attica,
12243 Athens,
Greece

INTRODUCTION

Water quality issues are of particular importance worldwide due to population growth, urbanization and industrialization, which have continuously stressed hydrological resources to the limits (Foley *et al.* 2005). Climate change is expected to impact negatively on water resources availability while at the same time water demand is expected to increase (Kanakoudis *et al.* 2017). As water demand is increasing rapidly, water systems are stressed by many factors (Kanakoudis & Karatzas 2017), the most hazardous of which is heavy metals release from industries, mining and alloy manufacturing. Heavy metals threaten the environment and public health, since they can accumulate, are not biodegradable, and cannot be metabolized or decomposed.

Moreover, exposure to heavy metals is a strong toxicity parameter in human health. Depending on the heavy metal, loss of memory, allergic reactions, high pressure, depression, irritability, aggressive behavior, insomnia, dyslexia, increased cholesterol, triglycerides, neuropathy and autoimmune diseases may affect human health (Falconer & Humpage 2005). Water is the most usual conductor to transfer heavy metals from almost all contamination sources to both the environment and humans. The toxicological effects depend on the chemical form and oxidation state of the metals (Mosivand *et al.* 2019). Therefore, reliable methods are needed to remove heavy metals from water (Daniel-da-Silva *et al.* 2008; Shen *et al.* 2009).

Research and applications in the fields of microfluidics and nanoparticles have attracted significant interest in recent years due to their unique advantages of micro-scale fluidic processes, combined with rapid advances in materials development. Microfluidics provides a great

doi: 10.2166/aqua.2020.090

opportunity to create devices capable of outperforming classical techniques in biomedical and chemical research (Convery & Gadegaard 2019).

Magnetic nanoparticles offer some attractive possibilities in water treatment. First, they have controllable sizes ranging from a few up to several tenths of nanometers, which places them at dimensions that are smaller than or comparable to those of a cell (10–100 μm), a virus (20–450 nm), a protein (5–50 nm) or a gene (2 nm wide and 10–100 nm long). This means that they can 'get close' to harmful substances. Indeed, they can be coated with molecules to make them interact with heavy metals (Inbaraj & Chen 2012). Second, the nanoparticles can be magnetic, which means that they can be manipulated by an external magnetic field (Karvelas *et al.* 2017b, 2018a). Third, the magnetic nanoparticles can be made to resonantly respond to a time-varying magnetic field, with advantageous results related to the transfer of energy from the existing field to the nanoparticle (Pankhurst *et al.* 2003).

Due to their small size, magnetic nanoparticles present properties that contribute to their extraordinary adsorption capacity and reactivity, both of which are favorable for the removal of heavy metal ions (Yang *et al.* 2019). In a ferrofluid, the magnetic particles can be influenced by an external magnetic field thus higher mixing efficiency between the ferrofluid and another sample solution can be obtained (Nouri *et al.* 2017). Furthermore research on ferrofluids indicates that Fe_2O_3 nanoparticles could improve the thermal resistance, and subsequently thermal performance, as well as the pipe's heat transfer coefficient, especially under the magnetic field (Goshayeshi *et al.* 2016). In this context, particles coated with special chemicals may be used to capture metal ions dissolved in water. Micromixers are used in order to obtain optimum chemical reactions for capturing heavy metals. Active micromixers can offer superior mixing compared to passive methods (Green *et al.* 2007) by using external disturbance to enhance the mixing process. Mixing of particles with water is very important and the most advanced idea in this field is the use of iron-core particles in conjunction with a magnetic micromixer. Apart from ion capture, another attractive property of magnetic particles is the possibility of separation of heavy metals captured by nanoparticles from water with the use of an external magnetic field. Also, an appropriate magnetic field can be applied to manage and control the flow behavior of fluids (Jamalabadi *et al.* 2018; Bagherzadeh *et al.* 2019). In addition, the presence of a magnetic field leads to an increase in the heat transfer coefficient at any mass concentration of the nanofluids (Malvandi *et al.* 2015; Arya *et al.* 2019) as well as it having effect on the magnetic convection of an electrically conducted fluid (Afrand *et al.* 2015). Several studies have been conducted with the use of guided magnetic particles in a microchannel (Karvelas *et al.* 2017b), with the results encouraging their effectiveness (Cai *et al.* 2017). Among them, Rida & Gijs (2004) describe the intense interaction between the fluid and the magnetic field by means of magnetic microchannel manipulation. Their approach is based on the dynamic movement of the structure of the beads held in a microfluidic stream, using a local alternating magnetic field, which causes rotational motion to the magnetic particles. Thus, a gradient of a time varied external magnetic field can be applied in a stream of water and magnetic nanoparticles flow in order to swirl particles and spread them all over the water almost uniformly to enhance and improve metal ion capture. Additional factors that influence the mixing efficiency are the geometry of the microchannel, and the inlet conditions such as velocity of the incoming fluids and entrance angle, as indicated in the literature. More specifically, the effect of the magnetic activation force by alternating the frequency and the lateral dimension of the channel was studied by Wang *et al.* (2008).

So far, our research has shown that for small velocity ratios between the two streams, one with the contaminated water and the other with the particulate water, no significant mixing is observed (Karvelas *et al.* 2019). Moreover, low mixing is found in the case of different entrance angles between the two streams, without the action of an external magnetic field (Karvelas *et al.* 2018b). In the present work, a numerical model is used for the investigation of mixing SPHERO magnetic particles (polystyrene) with the contaminated water under different magnetic field intensity, gradient and frequency. Simulations are employed in order to determine the optimal parameters for the magnetic field that will spread particles homogeneously in the water microchannel flow to achieve the maximum mixing efficiency, which will be necessary for particles to capture the impurities. In this study, the magnetic frequency effect on the

mixing efficiency is analyzed as compared with the magnitude and gradient of the magnetic field. The governing equations and important numerical details are presented in the Materials and Methods section, followed by the results of the present parametric study and, finally, the conclusions are presented.

MATERIAL AND METHODS

The slow water flow in a microfluidic duct is considered to be laminar and steady-state. The two water streams enter the domain from the upper and lower half of the inlet side for the contaminated and the nanoparticles filled streams, respectively. The configuration of the microchannel is shown in Figure 1. The continuity and the incompressible Navier–Stokes equation are solved for the water motion:

$$\nabla \cdot u = 0 \tag{1}$$

$$\rho\left(\frac{\partial u}{\partial t} + u \cdot \nabla u\right) = -\nabla p + \mu \nabla^2 u \tag{2}$$

where u is the velocity vector of the fluid, p is its pressure, t is the time, and ρ and μ are the density and dynamic viscosity of the fluid, respectively.

There are a wide range of forces that act on particles suspended in a fluid, but only a fraction of these forces are significant for nanofluids due to the small particle size (Karvelas *et al.* 2017a). In order to drive the particles into the microchannel, four major forces are taken into account (Figure 2): the magnetic force from the external time dependent magnetic field and the magnetic gradient force (Karvelas *et al.* 2017a), the nanoparticles are driven by the magnetic field, while the magnetic gradient may navigate the particles, and finally the contact forces among the aggregated nanoparticles and the wall. Also, for each particle the Stokes drag force and the gravitational forces due to gravity and buoyancy force are taken into account (Karvelas *et al.* 2017a).

The discrete motion of magnetic particles is governed by Newton's second law as:

$$m_i \frac{d\boldsymbol{u}_i}{dt} = \mathbf{F}_{\mathrm{mag},i} + \mathbf{F}_{\mathrm{hydro},i} + \mathbf{F}_{\mathrm{con},i} + \mathbf{F}_{\mathrm{grav},i} \tag{3}$$

$$I_i \frac{\partial \omega_i}{\partial t} = \mathbf{M}_{\mathrm{drag},i} + \mathbf{M}_{\mathrm{con},i} \tag{4}$$

where the index i stands for the ith-particle with diameter d_i, where $\mathbf{u}_i$ and ω_i are its transversal and rotational velocities, respectively, and m_i its mass. The mass moment of inertia matrix is I_i and the terms $\partial \boldsymbol{u}_i/\partial t$ and $\partial \omega_i/\partial t$ correspond to the linear and angular accelerations, respectively. $\mathbf{F}_{\mathrm{mag},i}$ and $\mathbf{F}_{\mathrm{hydro}}$ are the magnetic and the hydrodynamic forces, respectively. $\mathbf{F}_{\mathrm{con},i}$ stands for the normal and tangential contact forces, respectively. In addition, $\mathbf{F}_{\mathrm{grav},i}$ is the total force due to buoyancy and gravity. Furthermore, $\mathbf{M}_{\mathrm{drag},i}$ and $\mathbf{M}_{\mathrm{con},i}$ are the drag and contact moments, respectively. Moreover, the magnetic force at the magnetic particles is calculated (Karvelas *et al.* 2017a) by:

$$\mathbf{F}_{\mathrm{mag}} = V_p(\mathbf{m}_i \cdot \nabla)\boldsymbol{B}_0 \tag{5}$$

where V_p is the particle volume, $\mathbf{m}_i$ is the magnetic moment of particle i and $\boldsymbol{B}_0$ is the magnetic field which is

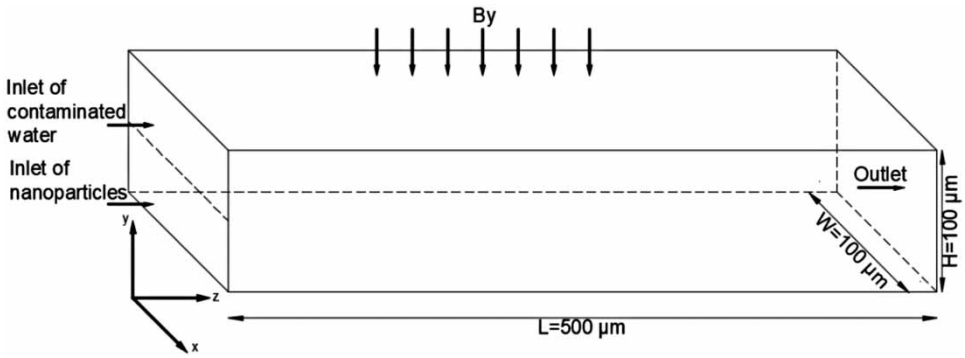

Figure 1 | Micromixer configuration and inflow/outflow conditions.

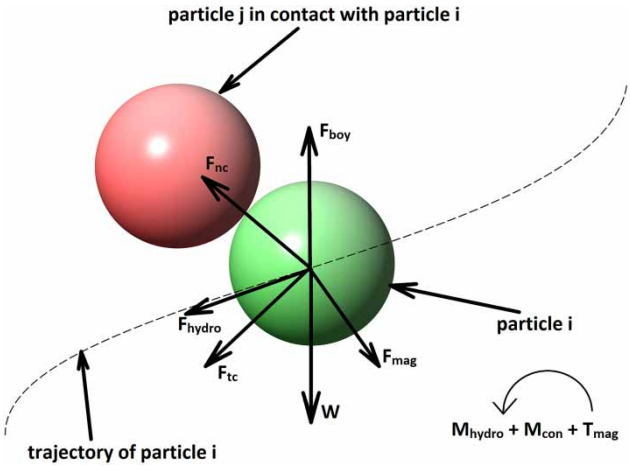

Figure 2 | Schematic diagram of the forces acting on particles (Lampropoulos *et al.* 2015).

generated by an external magnet. The magnetic moment $\mathbf{m}_i$ is given by:

$$\mathbf{m}_{\mathrm{i}} = \frac{4\pi}{\mu_0}\frac{\mu_r - 1}{\mu_r + 2}\frac{d_i^3}{8} \tag{6}$$

where μ_0 is the magnetic permeability of free space, and μ_r is the relative magnetic permeability of the particle. An external magnetic field consists of a time dependent part:

$$B_y = \mathbf{B_0}\sin(2\pi ft)$$

where $\mathbf{B_0}$ is magnitude, and f is frequency, and secondly by a magnetic gradient G_y aligned in the y direction that act together. Because the magnetic field is mainly in the y direction, B_x, B_z can be neglected and the corresponding magnetic actuation force is mostly along the y-direction.

Each particle is subjected to the fluid drag force. The drag force is given by:

$$\mathbf{F}_{\mathrm{hydro},i} = \frac{1}{2}\rho u_i^2 C_d A \tag{7}$$

where u_i is the velocity of the particle i relative to the fluid and A is the reference area which equals to πr^2, where r stands for the radius of the spherical particle. C_d is the drag coefficient given by:

$$C_d = \frac{24\,[1 + 0.15Re^{0.687}]}{Re} \tag{8}$$

where Re is the Reynolds number based on the particle diameter (Karimi *et al.* 2012). The contact force between the particles and the walls is calculated by using the discrete element method (DEM), which includes spring and damping models (Tijskens *et al.* 2003). The DEM is a numerical model capable of describing the mechanical behavior of assemblies of spheres and computing the motion and shear effect of a large number of small particles. In DEM, particles are approximated as rigid bodies and the interaction between them is explicitly considered. Only gravity and buoyancy are being included in the calculation of the body force. The gravitational force is addressed by:

$$\boldsymbol{F}_{\mathrm{grav},i} = W_i + F_{\mathrm{boy},i} = \frac{4}{3}\pi r_i^3(\rho_i - \rho)g \tag{9}$$

where ρ_i is the density of particle i, r_i is the radius of particle i and g is the acceleration due to gravity.

Parameters of simulations are selected based on the existing literature and are briefly presented in Table 1. More specifically, boundary conditions, dimensions of geometry, particles inlet flux and particle's density are based on the studies of Rida & Gijs (2004) and Karvelas *et al.* (2019). The length of the micromixer duct is $\mathrm{L} = 5\times10^{-4}$ m while its height and width are equal to $\mathrm{W} = \mathrm{H} = 1\times10^{-4}$ m, as depicted in Figure 1.

Table 1 | Simulation parameters

	Simulation parameters	
Dimensions of geometry	**Length (L): 5×10^{-4} m, height (H): 1×10^{-4} m, width (W): 1×10^{-4} m**	
Diameter of particles	1 μm	
Particles per second	3000	
Particle's density	1087 kg/cm^3	
Magnetic field (0.4,0.5,0.6) T	Frequency (5,10,15) Hz Magnitude of magnetic field (5,6,7,8) T/m	
	Boundary conditions	
Boundary	Velocity (U) (m/s)	Pressure (p) (pa)
Contaminated water (Vc)	0.0005	Zero gradient
Particle solution (Vp)	0.0005	Zero gradient
Outlet	Zero gradient	0
Walls	0	Zero gradient

The two water streams, the contaminated and the particles one, enter the micromixer from two different inlet ducts and are mixed in the duct (Figure 1) and then leave the microchannel from a common outlet. Contaminated water enters from the upper half inlet of the microchannel at a constant velocity of $U_0 = 5 \cdot 10^{-4}$m/s, while water with spherical magnetic particles enters from the lower half of the microchannel at the same velocity. On the wall of the microchannel, a no-slip boundary condition is applied. In addition, at the outlet of the microchannel, a constant pressure condition is applied.

The OpenFoam platform is used for the calculation of the flow field and the uncoupled equations of particles motion (Weller *et al.* 1998). The simulation process reads as follows: initially, the fluid flow is solved using the incompressible Navier–Stokes equations and the pressure correction method. Upon finding the steady-state flow field (pressure and velocity), the motion of particles is evaluated by a Lagrangian method. The implicit Euler method is used for solving Equations (3) and (4) and the time step for all numerical integration is 5×10^{-4} s in order to ensure the stability of the algorithm. The computational grid for the micromixer duct

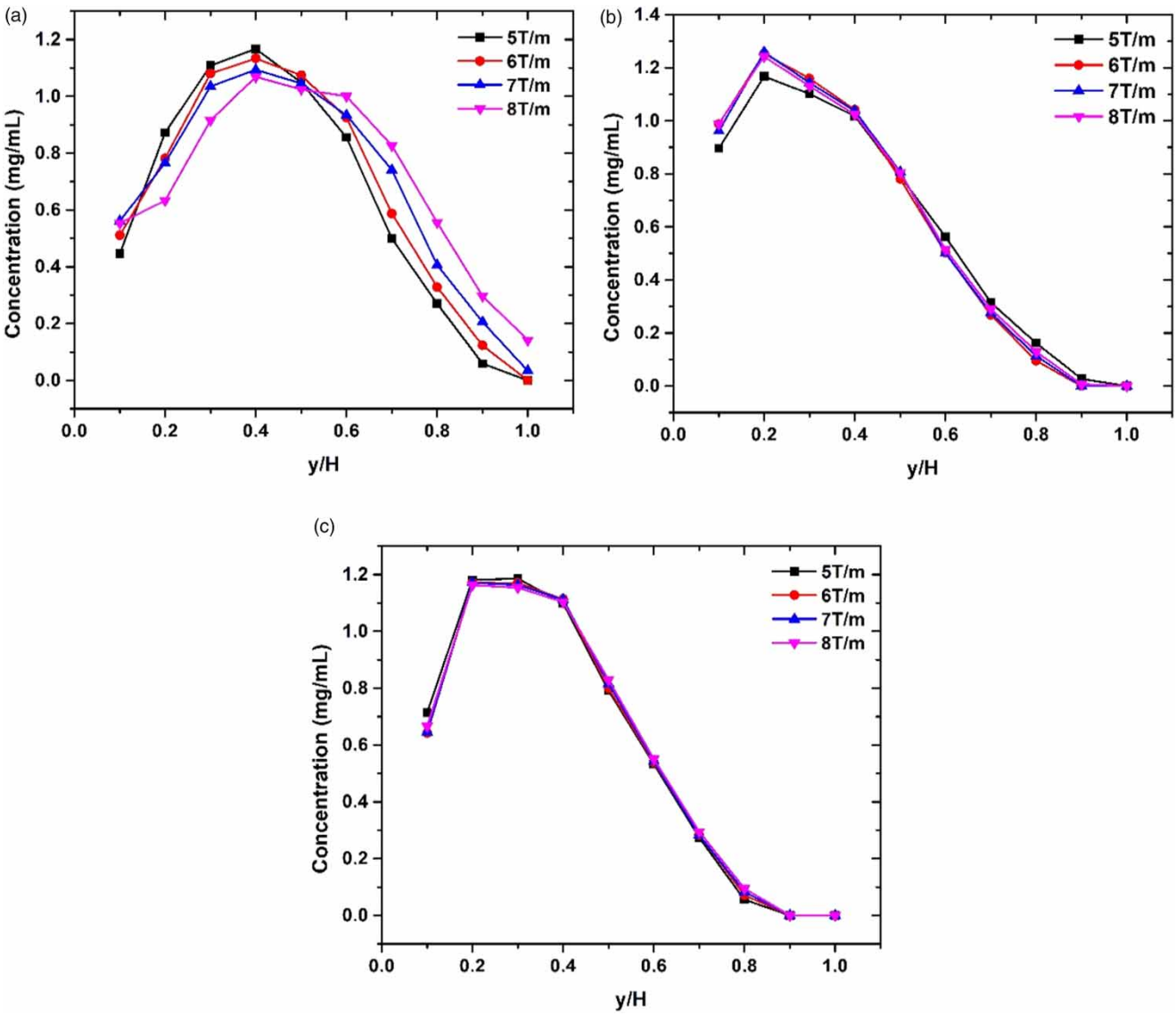

Figure 3 | Particles' concentration for $B_0 = 0.4$ T and different magnetic gradients for (a) $f = 5$ Hz, (b) $f = 10$ Hz, (c) $f = 15$ Hz.

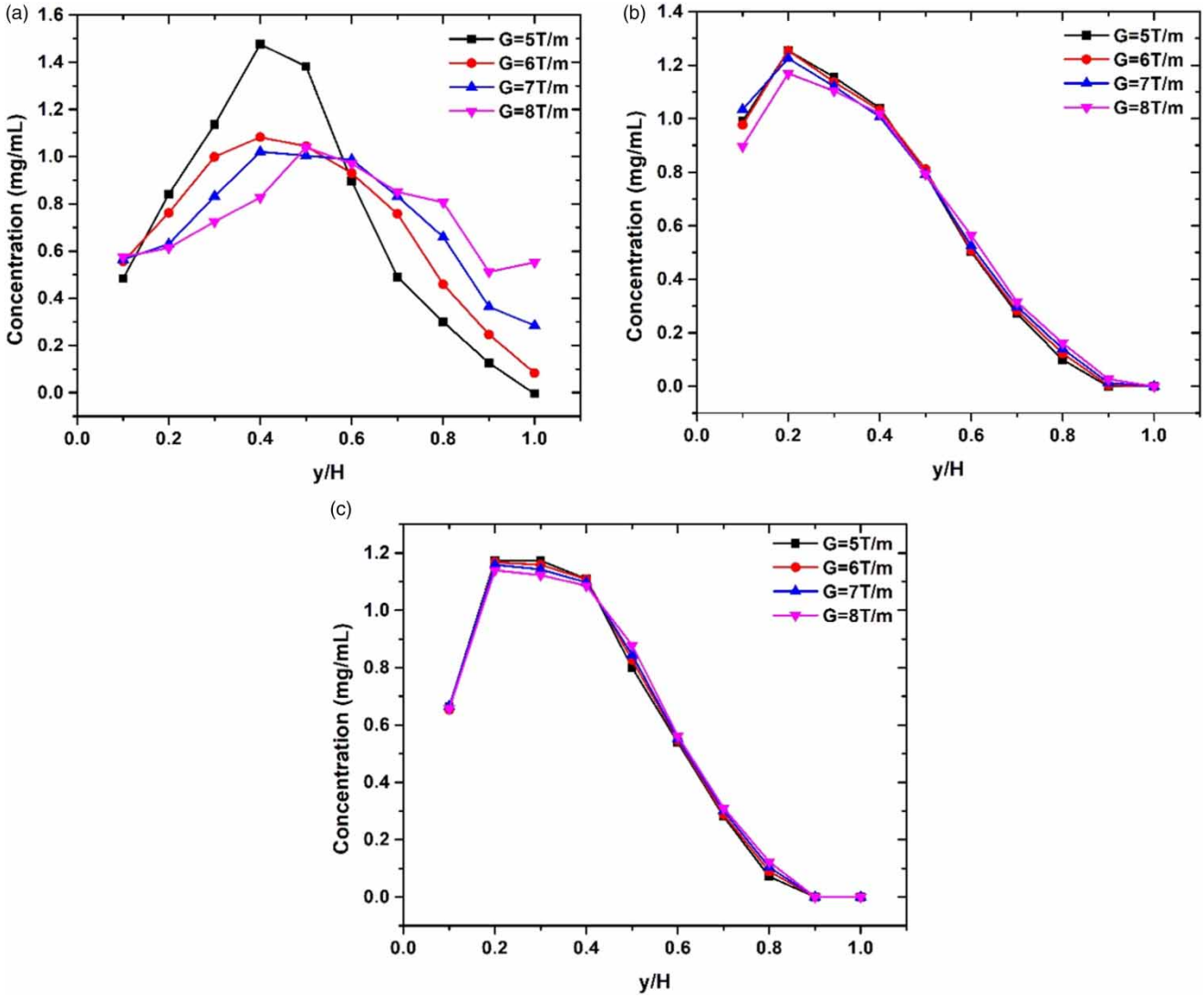

Figure 4 | Particles' concentration for $B_0 = 0.5$ T and different magnetic gradients for (a) $f = 5$ Hz, (b) $f = 10$ Hz, (c) $f = 15$ Hz.

that is studied here is composed of 13,650 cells which are adequate for the low Reynolds number of the current flow.

RESULTS AND DISCUSSION

Magnetic nanoparticles are found to form chains aligned to the magnetic field lines and drift under a magnetic gradient field (Karvelas *et al.* 2018a, 2018b). In the present work the external magnetic field is time varying, and thus no steady particle chains can be formed. Driven by the magnetic force, particles are expected to be shaken and thus be mixed inside the two water streams.

Our interest is on the particles' concentration profiles that should be as uniform as possible in the duct's cross-section for optimum mixing to be attained. Particulate spatiotemporal statistics are gathered for the mean concentration to be measured. As particles enter only from the lower part of the inlet, the temporal statistics are initiated after several eddy turn-over times (i.e. all particles to travel along the duct for several times) and only the last half part of the duct in the streamwise direction is used for the spatial statistics along with the spanwise direction. Then averaging

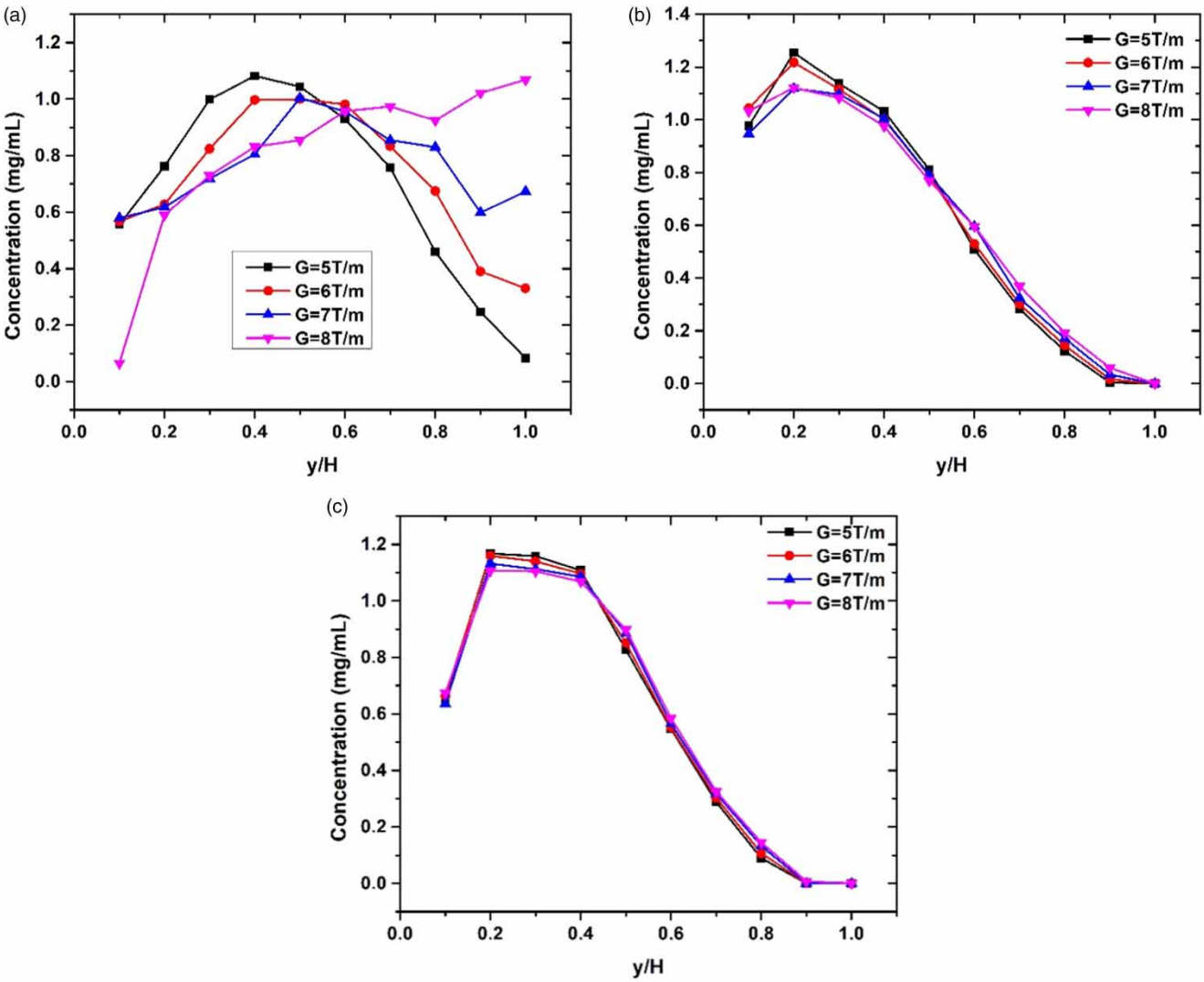

Figure 5 | Particles' concentration for $B_0 = 0.6$ T and different magnetic gradients for (a) $f = 5$ Hz, (b) $f = 10$ Hz, (c) $f = 15$ Hz.

process is repeated for several eddy turn-over times (and every five time steps), thus, statistics can be considered stationary in time and space.

Results of the present simulations are summarized in Figures 3–5 for the mean concentration (mg/mL) of particles for the dimensionless height of the duct, y/H, as the amplitude, gradient and frequency of the external magnetic field are varied. In present simulations, the magnetic gradient is kept positive in order to continuously drift particles from the lower part of the duct (where they are entering the domain) to the upper part (where contaminated water is found). Thus, the frequency of the time varied magnetic field is responsible for the periodic (up and down) shaking of the particles that may lead to mixing them with water everywhere in the duct.

Figure 3 summarizes the results from the particle concentration when the amplitude of the magnetic field is kept constant and equal to 0.4 T, its frequency is varied between 5 and 15 Hz and its gradient is varied in the range between 5 and 8 T/m, thus, a range which is easy to be found in the micrometer dimensions of the microfluidic ducts. Results for the case of $f = 5$ Hz are shown in Figure 3(a) where it is found that a large percentage of the particles are located between $0.2 < y/H < 0.6$ of the microchannel for most of the applied gradient fields. In this case, a nearly Gaussian distribution along y is observed. From Figure 3(b) and 3(c), it is

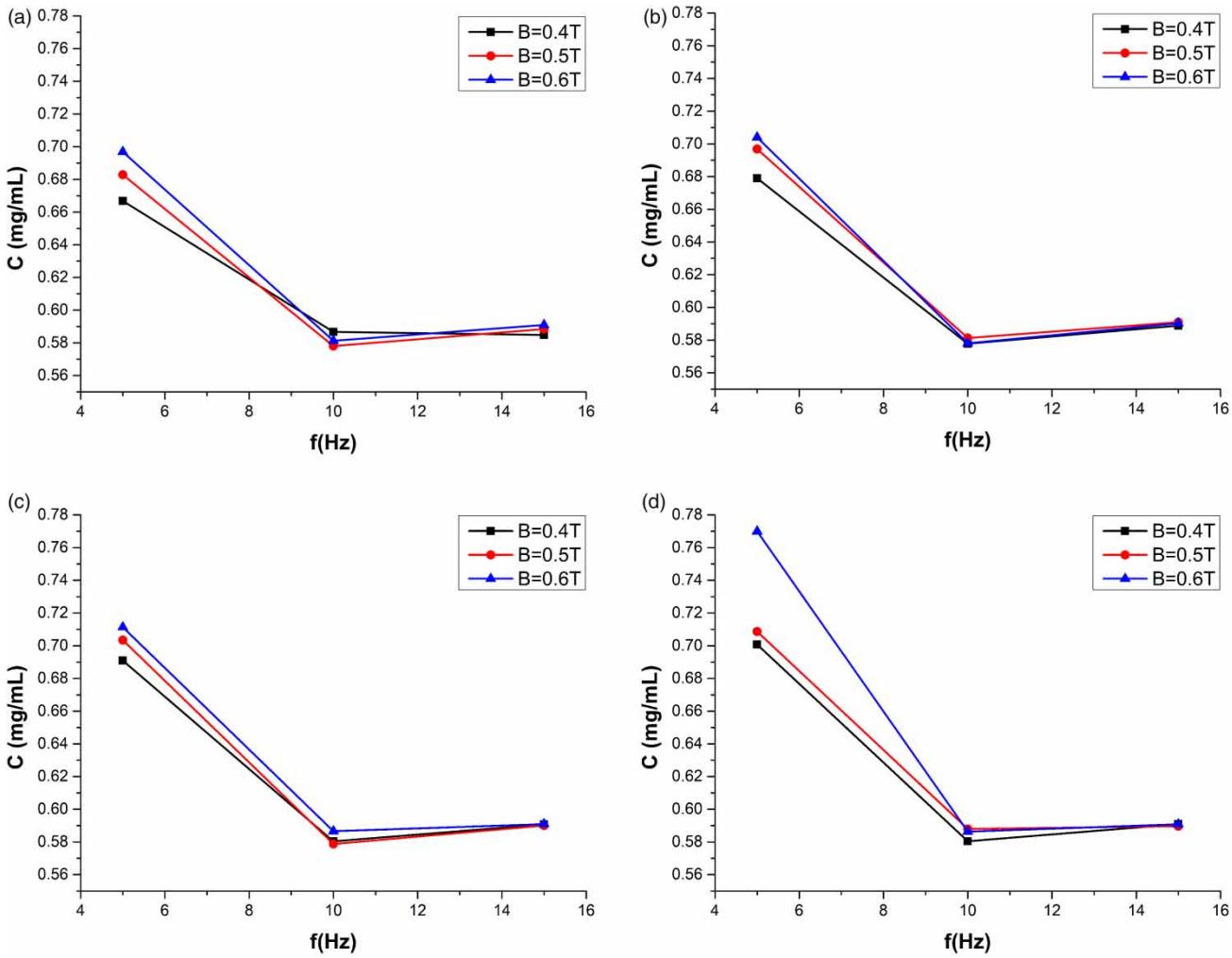

Figure 6 | Mean concentration for different magnitudes of the magnetic field B_0 for G equal to: (a) 5 T/m, (b) 6 T/m, (c) 7 T/m, and (d) 8 T/m.

obvious that as the frequency of the magnetic field increases, particles are mostly confined in the lower part of the duct and mixing is very poor. Moreover, it is found that as the frequency of the magnetic field increases, concentration profiles almost collapse for various gradient fields.

As the amplitude of the magnetic field increases from 0.5 and 0.6 T, as shown in the concentration profiles of Figures 4 and 5 respectively, the effects of the parameters studied here are following the same trend as in Figure 3. More specifically, under the lowest magnetic frequency value of 5 Hz, particles are spread more uniformly at most of the microchannel height. However, as frequency increases, particle confinement at the lower part of the duct increases because of their increased magnetic response in the fast temporal variation of the external forcing, i.e. they move quickly up and down without significant elevation. Figure 4(a) summarizes the concentration distribution of particles for amplitude 0.5 T and frequency 5 Hz, where the optimum distributions are found for the lowest gradient field.

The concentration profiles are shown in Figure 4(b) and 4(c) for the cases of $f = 10$ Hz and 15 Hz at 0.5 T, respectively, and for the same frequencies but for 0.6 T are shown in Figure 5(b) and 5(c), respectively. The general picture in all these cases is like that in the case of 0.4 T of Figure 3 as the magnetic amplitude is increased, thus, as particles translate due to the water flow and move out of the duct only minor elevation is succeeded. It is found that as the frequency of the magnetic field increases, the particles are localized in a

narrower region of the height of the microchannel, and this distribution does not vary significantly with increasing gradient, at least for the range of values studied here. Thus, the large percentage of the particles are located between $0.2 < y/H < 0.3$ of the microchannel height for 0.4 T, between $0.3 < y/H < 0.4$ for the amplitude of 0.5 T and between $0.3 < y/H < 0.4$ for the amplitude of 0.6 T.

In order to quantify the effects due to magnitude, gradient and frequency of the magnetic field, the present results are compared against the optimum concentration needed by particles to distribute homogeneously at the volume of the duct, i.e. 0.85 mg/mL in the specific configuration. The difference between the present results and the optimum concentration may be considered as a purification indicator, i.e. the potential of the particles to absorb heavy metals. By integration, this difference can be considered as a measure of the quality of mixing due to magnetic field. The mean concentration of the present cases after integration are summarized in Figure 6, where the horizontal axis represents the frequency and the vertical axis represents the mean concentration C (in mg/mL). It is found that as the magnetic frequency decreases, more homogeneous particles distributions are observed, since the mean concentration C increases. Moreover, as the magnetic field's magnitude increases, the mean concentration C increases and the only secondary effects are due to magnetic gradient increase. Among the present results, the better distribution is achieved for the combination of 0.6 T, 8 T/m, and 5 Hz of the magnitude, gradient and magnetic frequency, respectively, which is equal to $C = 0.77$ mg/mL.

Summarizing our findings, we can see that lower frequencies of the magnetic field result in more homogeneous distributions of the particles across the whole height of the duct and this occurs in all cases, independently of the amplitude of the field and the magnetic gradient, at least for the ranges of values studied here. Among these cases (with a lower frequency) there are some where a more homogenous distribution takes place for given values of magnetic field, these cases are mostly connected to higher external magnetic gradients due to its ability to stronger elevate the particles. The fluctuation which was observed for lower frequencies (5 Hz) was caused by the available time which the particles could move in the duct at y direction. As the frequency increases, the necessary time which must move in the duct (either up or down) is decreasing, so the particles are localized and not distributed.

CONCLUSIONS

The use of magnetic particles in the possible capture of heavy metal ions from contaminated water in microfluidics is considered here. The mixing of two water streams, the contaminated and the particulate one, are studied under various external magnetic configurations. The magnitude of a magnetic gradient and the amplitude and frequency of a time varied magnetic field are applied together at the microduct. It is primarily found that the lower the frequency is, the better the distribution of the particles in the flow duct will be. Thus, for the lower frequency of 5 Hz, the mean concentration of particles was found more than two times higher as frequency increased to 10 and 15 Hz. Moreover, as the magnitude of the magnetic gradient increases, more homogeneous particle distributions are found and the same is observed for the increase of the amplitude of the magnetic field. The optimum combination is found to be for 0.6 T, 8 T/m and 5 Hz which is equal to $C = 0.77$ mg/mL. The present results are very promising for the further development of the method and will relate to the chemical kinetics of the coatings-ions reaction.

ACKNOWLEDGEMENTS

The authors are grateful to Greek Research & Technology Network (GRNET) for the computational time granted in the National HPC facility ARIS.

REFERENCES

Afrand, M., Sina, N., Teimouri, H., Mazaheri, A., Safaei, M. R., Esfe, M. H., Kamali, J. & Toghraie, D. 2015 Effect of magnetic field on free convection in inclined cylindrical annulus containing molten potassium. *Int. J. Appl. Mech.* **7** (4), 1550052.

Arya, H., Sarafraz, M. M. & Arjomandi, M. 2019 Pool boiling under the magnetic environment: experimental study on the role of magnetism in particulate fouling and bubbling of iron oxide/ethylene glycol nano-suspension. *Heat Mass Transf.* **55** (1), 119–132.

Bagherzadeh, S. A., Jalali, E., Sarafraz, M. M., Akbari, O. A., Karimipour, A., Goodarzi, M. & Bach, Q. V. 2019 Effects of magnetic field on micro cross jet injection of dispersed nanoparticles in a microchannel. *Int. J. Numer. Methods Heat Fluid Flow* **30** (5), 2683–2704. doi:10.1108/HFF-02-2019-0150.

Cai, G., Xue, L., Zhang, H. & Lin, J. 2017 A review on micromixers. *Micromachines* **8** (9), 274.

Convery, N. & Gadegaard, N. 2019 30 years of microfluidics. *Micro Nano Eng.* **2**, 76–91.

Daniel-da-Silva, A. L., Lóio, R., Lopes da Silva, J., Trindade, T., Goodfellow, B. & Gil, A. 2008 Effects of magnetite nanoparticles on the thermorheological properties of carrageenan hydrogels. *J. Colloid Interface Sci.* **324** (1–2), 205–211.

Falconer, I. & Humpage, A. R. 2005 Health risk assessment of cyanobacterial (blue-green algal) toxins in drinking water. *Int. J. Environ. Res Public Health* **2** (1), 43–50.

Foley, A. J., Defries, R., Asner, G., Barford, C., Bonan, G., Carpenter, S., Chapin, F. S., Coe, M., Daily, G., Gibbs, H., Helkowski, J. H., Holloway, T., Howard, E. A., Kucharik, C., Monfreda, C., Patz, J., Prentice, I., Ramankutty, N. & Snyder, P. K. 2005 Global consequences of land use. *Science* **309** (5734), 570–574.

Goshayeshi, H. R., Goodarzi, M., Safaei, M. R. & Dahari, M. 2016 Experimental study on the effect of inclination angle on heat transfer enhancement of a ferrofluid in a closed loop oscillating heat pipe under magnetic field. *Exp. Therm. Fluid Sci.* **74**, 265–270.

Green, J., Holdø, A. & Khan, A. 2007 A review of passive and active mixing systems in microfluidic devices. *Int. J. Multiphys.* **1**, 1–32.

Inbaraj, B. S. & Chen, B. H. 2012 In vitro removal of toxic heavy metals by poly (γ-glutamic acid)-coated superparamagnetic nanoparticles. *Int. J. Nanomed.* **7**, 4419–4432.

Jamalabadi, M. Y. A., Daqiqshirazi, M., Nasiri, H., Safaei, M. R. & Nguyen, T. K. 2018 Modeling and analysis of biomagnetic blood Carreau fluid flow through a stenosis artery with magnetic heat transfer: a transient study. *PLoS ONE* **13** (2), 0192138.

Kanakoudis, V. & Karatzas, G. 2017 Efficient and sustainable water systems management toward worth living development. *Environ. Sci. Pollut. Res.* **24** (25), 20,119–20,121.

Kanakoudis, V., Tsitsifli, S., Papadopoulou, A., Curk, B. & Karleusa, B. 2017 Water resources vulnerability assessment in Adriatic Sea region: the case of Corfu Island. *Environ. Sci. Pollut. Res.* **24**, 20,173–20,186.

Karimi, M., Akdogan, G., Dellimore, K. H. & Bradshaw, S. M. 2012 Comparison of different drag coefficient correlations in the CFD modelling of a laboratory-scale Ruschton-Turbine floatation tank. In: *Ninth International Conference on CFD in the Minerals and Process Industries*. Available from: www.cfd.com.au/cfd_conf12/PDFs/039KAR.pdf (accessed 8/11/2019).

Karvelas, E. G., Lampropoulos, N. K. & Sarris, I. E. 2017a A numerical model for aggregations formation and magnetic driving of spherical particles based in OpenFOAM®. *Comput. Methods Programs Biomed.* **142**, 21–30.

Karvelas, E. G., Lampropoulos, N. K., Karakasidis, T. E. & Sarris, I. E. 2017b A computational tool for the estimation of the optimum gradient magnetic field for the magnetic driving of the spherical particles in the process of cleaning water. *Desalination Water Treat.* **99**, 27–33.

Karvelas, E. G., Karakasidis, T. E. & Sarris, I. E. 2018a Computational analysis of paramagnetic spherical Fe_3O_4 nanoparticles under permanent magnetic fields. *Comput. Mater. Sci.* **154**, 464–471.

Karvelas, E., Liosis, C., Karakasidis, T. & Sarris, I. 2018b Mixing of particles in micromixers under different angles and velocities of the incoming water. *Proceedings.* **2**, 577. 10.3390/proceedings2110577.

Karvelas, E. G., Liosis, C., Benos, L., Karakasidis, T. E. & Sarris, I. E. 2019 Micromixing efficiency of particles in heavy metal removal processes under various inlet conditions. *Water* **11** (6), 1135.

Lampropoulos, N. K., Karvelas, E. G. & Sarris, I. E. 2015 Computational study of the particles interaction distance under the influence of steady magnetic field. *Advances in Systems Science and Applications* **153** (3), 233–241.

Malvandi, A., Safaei, M. R., Kaffash, M. H. & Ganji, D. D. 2015 MHD mixed convection in a vertical annulus filled with Al_2O_3–water nanofluid considering nanoparticle migration. *J. Magn. Magn. Mater.* **382**, 296–306.

Mosivand, S., Kazeminezhad, I. & Fathabad, S. P. 2019 Easy, fast, and efficient removal of heavy metals from laboratory and real wastewater using electrocrystalized iron nanostructures. *Microchem. J.* **146**, 534–543.

Nouri, D., Zabihi-Hesari, A. & Passandideh-Fard, M. 2017 Rapid mixing in micromixers using magnetic field. *Sens. Actuators A Phys.* **255**, 79–86.

Pankhurst, Q. A., Connolly, J., Jones, S. K. & Dobson, J. 2003 Applications of magnetic nanoparticles in biomedicine. *J. Phys. D Appl. Phys.* **36**, R167.

Rida, A. & Gijs, M. A. M. 2004 Dynamics of magnetically retained supraparticle structures in a liquid flow. *Appl. Phys. Lett.* **85**, 4986–4988.

Shen, Y., Tang, J., Nie, Z., Wang, Y., Ren, Y. & Zuo, L. 2009 Preparation and application of magnetic Fe_3O_4 nanoparticles for wastewater purification. *Separ. Purif. Technol.* **25**, 312–319.

Tijskens, E., Ramon, H. & Baerdemaeker, J. 2003 Discrete element modelling for process simulation in agriculture. *J. Sound Vibration* **266**, 493–514.

Wang, Y., Zhe, J., Chung, B. T. F. & Dutta, P. 2008 A rapid magnetic particle driven micromixer. *Microfluid. Nanofluidics* **4**, 375–389.

Weller, H. G., Tabor, G., Jasak, H. & Fureby, C. 1998 A tensorial approach to computational continuum mechanics using object-oriented techniques. *Comput. Phys.* **12**, 620–631.

Yang, J., Hou, B., Wang, J., Tian, B., Bi, J., Wang, N., Li, X. & Huang, X. 2019 Nanomaterials for the removal of heavy metals from wastewater. *Nanomaterials* **9**, 424.

First received 15 June 2019; accepted in revised form 26 January 2020. Available online 18 February 2020